Intestinal inflammation modulates the expression of ACE2 and TMPRSS2 and potentially overlaps with the pathogenesis of SARS-CoV-2 related disease

Mayte Suárez-Fariñas[+1,2], Minami Tokuyama[+3,4], Gabrielle Wei[1,2], Ruiqi Huang[1,2], Alexandra Livanos[3,4], Divya Jha[3,4], Anais Levescot[5,6], Roman Kosoy[1,2], Haritz Irizar[7], Sascha Cording[5,6], Wenhui Wang[1,2], Ryan Ungaro[3], Antonio Di'Narzo[1,2], Gustavo Martinez[3,4], Maria Suprun[1], Michael J. Corley[8], Aleksandar Stojmirovic[9], Sander M. Houten[1,2], Mark Curran[9], Carrie Brodmerkel[9], Jacqueline Perrigoue[9], Joshua R. Friedman[9], Ke Hao[1,2], Eric E. Schadt[1,2], Jun Zhu[1,2], Huaibin M. Ko[11], Judy Cho[2,3,10], Marla C. Dubinsky[3], Bruce E. Sands[3,] Lishomwa Ndhlovu[8], Nadine Cerf-Benssusan[5,6], Andrew Kasarskis[1,2], Jean Frederic Colombel[3,4], Noam Harpaz[11], Carmen Argmann*[1,2], Saurabh Mehandru*[3,4]

Affiliations:

[1]Center for Biostatistics, Department of Population Health Science and Policy, Icahn School of Medicine at Mount Sinai, New York, NY, USA
[2]Icahn Institute for Data Science and Genomic Technology, New York City, NY, USA
[3] The Dr. Henry D. Janowitz Division of Gastroenterology, Department of Medicine, Icahn School of Medicine at Mount Sinai, New York, NY, USA
[4] Precision Institute of Immunology, Icahn School of Medicine at Mount Sinai, New York, NY, USA
[5]Inserm, UMR1163, Laboratory of Intestinal Immunity and Institute Imagine, Paris, France.
[6]Université de Paris, Paris, France
[7]University College London, Department Mental Health Sciences Unit, London, UK
[8] Division of Infectious Diseases, Department of Medicine, Weill Cornell Medicine, New York, NY, USA
[9] Janssen R&D, Spring House, PA, USA
[10]The Charles Bronfman Institute of Personalized Medicine, Icahn School of Medicine at Mount Sinai, New York, NY, USA
[11]Department of Pathology, Icahn School of Medicine at Mount Sinai, New York, NY, USA

+ Contributed equally

* Address correspondence to saurabh.mehandru@mssm.edu and carmen.argmann@mssm.edu

Author contributions: SM, AC, MSF, MT, GW and DJ drafted the manuscript. SM, AC and MSF designed the study, supervised experimental data collection and coordinated integration of collaboration between all participating laboratories. MT performed immunostaining experiments. GW performed network analysis experiments and RH performed statistical analyses. WW, AD, KH, JZ were involved in various aspects of data generation, curation or analysis. All authors critically reviewed and edited the final version of the manuscript.

Competing interests: SM and JFC have an unrestricted, investigator-initiated grant from Takeda Pharmaceuticals to examine novel homing mechanisms to the GI tract. RCU has served as an advisory board member or consultant for Eli Lilly, Janssen, Pfizer and Takeda. Mount Sinai co-authors (from Genetics and Genomics, Icahn Institute for Data Science and Genomic Technology, Human Immune Monitoring Center, Population Health Science and Policy, Division of Gastroenterology, Pediatric GI and Hepatology, Susan and Leonard Feinstein IBD Clinical Center at Icahn School of Medicine at Mount Sinai) were partially funded as part of research alliance between Janssen Biotech and The Icahn School of Medicine at Mount Sinai. MC, AS, JP and CB are employees at Research and Development. and JRF is a former employee at Janssen Research and Development and is currently employed at Alnylam Pharmaceuticals. MD is a consultant for Janssen. BES discloses consulting fees from 4D Pharma, Abbvie, Allergan, Amgen, Arena Pharmaceuticals, AstraZeneca, BoehringerIngelheim, Boston Pharmaceuticals, Capella Biosciences, Celgene, Celltrion Healthcare, EnGene, Ferring, Genentech, Gilead, Hoffmann-La Roche, Immunic, Ironwood Pharmaceuticals, Janssen, Lilly, Lyndra, MedImmune, Morphic Therapeutic, Oppilan Pharma, OSE Immunotherapeutics, Otsuka, Palatin Technologies, Pfizer, Progenity, Prometheus Laboratories, Redhill Biopharma, Rheos Medicines, Seres Therapeutics, Shire, Synergy Pharmaceuticals, Takeda, Target PharmaSolutions, Theravance Biopharma R&D, TiGenix, Vivelix Pharmaceuticals; honoraria for speaking in CME programs from Takeda, Janssen, Lilly, Gilead, Pfizer, Genetech; research funding from Celgene, Pfizer, Takeda, Theravance Biopharma R&D, Janssen. MCD discloses consulting fees from Abbvie, Allergan, Amgen, Arena Pharmaceuticals, AstraZeneca, BoehringerIngelheim, Celgene, Ferring, Genentech, Gilead, Hoffmann-La Roche, Janssen, Pfizer, Prometheus Biosciences, Takeda, Target PharmaSolutions and research funding from Abbvie, Janssen, Pfizer, Prometheus Biosciences Takeda. Dr. Colombel reports receiving research grants from AbbVie, Janssen Pharmaceuticals and Takeda; receiving payment for lectures from AbbVie, Amgen, Allergan, Inc. Ferring Pharmaceuticals, Shire, and Takeda; receiving consulting fees from AbbVie, Amgen, Arena Pharmaceuticals, Boehringer Ingelheim, Celgene Corporation, Celltrion, Eli Lilly, Enterome, Ferring Pharmaceuticals, Geneva, Genentech, Janssen Pharmaceuticals, Landos, Ipsen, Imedex, Medimmune, Merck, Novartis, O Mass, Otsuka, Pfizer, Shire, Takeda, Tigenix, Viela bio; and holds stock options in Intestinal Biotech Development and Genfit.

Abstract:

Immune dysregulation and cytokine release syndrome have emerged as pathological hallmarks of severe Coronavirus Disease 2019 (COVID-19), leading to the evaluation of cytokine antagonists as therapeutic agents. A number of immune-directed therapies being considered for COVID-19 patients are already in clinical use in chronic inflammatory conditions like inflammatory bowel disease (IBD). These considerations led us to systematically examine the intersections between COVID-19 and the GI tract during health and intestinal inflammation. We have observed that IBD medications, both biologic and non-biologic, do not significantly impact ACE2 and TMPRSS2 expression in the uninflamed intestines. Additionally, by comparing SARS CoV2-induced epithelial gene signatures with IBD-associated genes, we have identified a shared molecular subnetwork between COVID-19 and IBD. These data generate a novel appreciation of the confluence of COVID-19- and IBD-associated inflammation and provide mechanistic insights supporting further investigation of specific IBD drugs in the treatment of COVID-19.

Introduction

Severe acute respiratory syndrome Coronavirus 2 (SARS-CoV-2) and the ensuing coronavirus Disease 2019 (COVID-19)[1], have evolved into a global pandemic[2]. The common symptoms of COVID-19 include fever, cough, and shortness of breath within 2 to 14 days after exposure[3]. About a third of COVID-19 patients also report gastrointestinal (GI) symptoms, comprising loss of appetite, diarrhea, vomiting, nausea or abdominal pain[4-7]. Immunopathology has been suggested as a primary driver of morbidity and mortality with COVID-19. Most notably, elevated IL-6 levels are associated with ICU admission, respiratory failure, and poor prognosis[8]. Reports that other major proinflammatory cytokines (TNF-α, IFN-ɣ, IL-2) are elevated underscore a potentially pathogenic $T_H1/2$ program in COVID-19[9].

Angiotensin converting enzyme-2 (ACE2) is a carboxypeptidase that catalyzes the conversion of angiotensin I into angiotensin 1-9, and angiotensin II into angiotensin 1-7[10-13]. ACE2 can also be cleaved by serine proteases such as transmembrane serine protease (TMPRSS) 2, TMPRSS11D and TMPRSS1. Early events in the pathogenesis of SARS-CoV-2 infection include attachment of the receptor binding domain of the viral spike (S) protein to epithelial ACE2[14-17]. The S protein is then cleaved by TMPRSS2, which facilitates viral entry into the cytoplasm of the host cell[14].

Inflammatory bowel diseases (IBD) encompassing Crohn's disease (CD) and ulcerative colitis (UC) are chronic, inflammatory disorders of the GI tract that are treated with conventional immunosuppressive drugs such as corticosteroids, biologic therapies and immunomodulatory drugs[18, 19]. Given that SARS-CoV-2 co-opts receptors expressed by mucosal epithelial cells, COVID-19 has the potential to intersect with the pathogenesis of IBD and by extension, its treatment, at a number of points[20, 21]. For example, pro-inflammatory cytokines such as interferons (IFN) enhance ACE2 expression[22], which therefore could increase in response to gut inflammation. Conversely, immunomodulatory drugs used in IBD therapeutics[18, 19] could potentially be used in COVID-19 patients to manage the "cytokine storm" associated with severe disease.

Therefore, in this study we systematically examined potential areas of intersection between the uninflamed and inflamed GI tract and COVID-19 disease. The results of this study may improve our molecular understanding of how COVID-19 intersects IBD and may provide a rationale for further investigation of drugs used in IBD therapeutics for use in patients with COVID-19.

Methods

Immunofluorescence microscopy:

Specimens were obtained via clinical endoscopy during routine care (Table S1,S2). Tissue was formalin fixed and paraffin embedded by the clinical pathology core at our institution. Primary antibodies used

included ACE2 (abcam-ab15348, 1:1000), EPCAM (abcam-ab228023, prediluted) and mouse anti-TMPRSS2 (Millipore-MABF2158, 1:500) and staining was performed as detailed in supplementary methods.

Study cohorts:

Cross sectional cohorts:

1. The Mount Sinai Crohn's and Colitis Registry (MSCCR)

Gene expression data was obtained from a cross sectional cohort (~1200 patients) who were enrolled in the Mount Sinai Crohn's and Colitis Registry (MSCCR) between December 2013 and September 2016 via a protocol approved by the Icahn School of Medicine at Mount Sinai Institutional Review Board. Informed consent was obtained from all participants recruited into the study. The clinical and demographic information was obtained through an extensive questionnaire (ST3). Analysis of the MSCCR cohort is detailed in supplementary methods.

2. The RISK cohort[23]: ACE2 and TMPRSS2 in treatment-free pediatric CD (<17 years of age) patients was studied using RNA-seq expression profiles from GSE57945, which includes ileal biopsies from endoscopically defined inflamed samples (n=160), non-inflamed (n=53) and non-IBD controls (n=42).

2. **Longitudinal Cohorts:**

ii) The GSE100833 series included samples from 80 anti-TNFa refractory CD patients enrolled in a phase 2b crossover trial (CERTIFI trial) as described previously[24] and detailed in supplementary methods.

iii)The GSE73661 series. This cohort included gene expression profiles (Affymetrix Human Gene 1.0 ST arrays) from colonic biopsies from moderate-to-severe UC patients enrolled in two trials that evaluated the efficacy of vedolizumab (GEMINI-I and GEMINI LTS) in UC patients[25] as detailed in supplementary methods.

MSCCR Bayesian regulatory gene network (BGRN) generation:

BRGNs can capture fundamental properties of complex systems in states that give rise to complex (diseased) phenotypes[24]. BGRNs were generated from RNA sequence data generated on intestinal biopsies from the MSCCR cohort using their intestinal expression QTL information (eQTLs) as priors. The BGRNs were region- (ileum or colon/rectum) and disease- (CD, UC, and control) specific and included both inflamed and uninflamed biopsies and were constructed using RIMBAnet software[24] and visualized using Cytoscape 3.7[26]. We also used two publicly available BGRNs from the RISK and the CERTIFI cohort[24]. See supplementary methods for further details.

Bayesian subnetwork generation:

ACE2 and TMPRSS2 subnetworks: Gene-centric subnetworks were generated by selecting either ACE2 or TMPRSS2 on various BGRNs and expanding out three to five layers (undirected) to obtain the nearest ACE2 or TMPRSS2 neighbors. The connected subnetworks obtained were generally between 200-500 genes in total.

IBD inflammation- and Epithelial Model-SARS-CoV-2-*infection- associated subnetwork*s: MSCCR IBD inflammation genes were defined as differentially expressed genes (FDR<0.05 and fold change>2) between IBD inflamed and non-inflamed samples contrasted in a mixed-effect model with a random intercept for each patient and fixed factors for tissue, region and disease as well as core technical and demographic covariates.

We curated molecular signatures associated with COVID-19 response in various epithelial model systems recently published[27, 28]. SARS-CoV-2 infection of: i) A549 lung alveolar carcinoma cells and normal human bronchial epithelium (NHBE) for 24 hours[27] or ii) human small intestinal organoids (hSIOs) grown in either Wnt high expansion medium (EXP) or differentiation medium (DIF)[28].

*IBD drug response-associated subnetwork*s:

Gene signatures representing the response to infliximab and ustekinumab in gut biopsies of CD patients were generated using publicly available data. The GSE16879[29] series was used to generate an ileal gene expression signature of infliximab response as defined by endoscopic and histologic findings at 4-6 weeks post-treatment. For the ustekinumab signature, the series GSE112366[30] including microarray expression profiles from biopsies of moderate-to-severe CD patients enrolled in two phase 3 studies (UNITI-2 and IM-UNITI) were used. Ileal biopsies from responders were compared to baseline using the *limma* framework.

Genes found altered in NHBE/A549 or organoids following SARS-CoV-2 infection[27]; IBD inflammation; or response to medications were separately projected onto various BGRNs allowing for 1 nearest neighbor. The most connected subnetworks were then extracted to generate model-specific SARS-CoV-2 infection-; IBD inflammation-; or drug-response associated subnetworks. Genes common between these networks were determined and tested for enrichment to various genesets using the Fisher's exact test and p-values were adjusted using Benjamini-Hochberg (BH) procedure.

Pathway and geneset enrichment analysis of subnetworks:

Gene subnetworks were tested for functional enrichment using a Fisher's exact test with BH multiple test correction on a collection of gene sets. The collection of gene sets included i) Reactome pathways sourced from Enrichr[31], i) genesets from Smillie et al[32], ii) Huang et al[33], iii) various macrophage perturbations (e.g. cytokines)[34], iv) ACE2 co-expressed genes[35] and v) reported IBD GWAS genes (see supplementary methods).

Key driver gene analysis:

Key driver analysis (KDA) identifies key or "master" driver genes for a given gene set in a given BGRN. We used a previously described KDA algorithm[36] which is summarized in supplementary methods. Genesets for KDA included those associated with NHBE-COVID-19 infection or IBD inflammation. Key driver genes (KDGs) were summarized by frequency across the networks/genesets tested.

Geneset variation analysis of SARS-CoV-2-infection gene expression signatures:

We employed the epithelial model-COVID-19 response gene signatures (adjusted p value <0.05) in a gene set variation analysis (GSVA) using gene expression data from MSCCR and CERTIFI cohorts. For each gene set (up or down-regulated), GSVA was used to obtain a sample-wise enrichment score, that were then used for hypothesis testing with respect to phenotype information.

Results

Healthy gut segments express ACE2 and TMPRSS2 proteins

To define the localization and distribution of ACE2, immunofluorescence (IF) microscopy was performed on histologically normal GI tissue in 20 adults (9 males, 11 females) and 7 children (4 males, 3 females) (Figure 1 and Table S1). ACE2 expression was observed on the small intestinal surface epithelium in all subjects in a continuous distribution with the exception of occasional breaks representing the mucin from goblet cells (Figure 1a-b). In all examined small intestinal segments, ACE2 could be detected on the crypt epithelium, though to a lesser extent than on the surface epithelium. TMPRSS2 expression was less abundant in the small bowel, and when detectable, was exclusively found on crypt epithelium (Figure S1a-b)

In the colon, ACE2 expression was patchy and could not be identified in every subject, in contrast to the small bowel (Figure 1c). This inconsistency across different donors could not be readily associated with age, sex, ACE inhibitor treatment, nor the colonic segment being examined. In contrast, TMPRSS2 expression was more robust in the colon and was readily detectable on both surface and crypt epithelia (Figure S1c). Thus, the healthy gut expresses more ACE2 protein in the ileum compared to the colon and more TMPRSS2 protein in the colon compared to the ileum.

ACE2 and TMPRSS2 mRNA expression varies in healthy or inflamed gut segments

Next, we examined ACE2 and TMPRSS2 mRNA levels in the intestine of non-IBD controls and IBD patients with active and inactive disease enrolled in MSCCR (Table S3). Consistent with the protein data, ACE2 gene expression was higher in the uninflamed ileum compared to the uninflamed colon or rectum. With inflammation, ileal ACE2 mRNA expression was significantly decreased compared to either uninflamed biopsies from IBD patients or non-IBD controls. In contrast, in the rectum ACE2 mRNA

expression was increased with inflammation when compared to the uninflamed IBD patients or non-IBD controls (Figure 2a, upper panels). There were no significant differences between the expression in UC versus CD patients. We further validated these results using the pediatric IBD RISK cohort[23] where ACE2 mRNA was significantly decreased in the ileum of patients with active IBD as well (Figure 2b).

The expression of TMPRSS2 in the MSCCR cohort was moderately higher in the colon compared to ileum. In both ileum and colon biopsies TMPRSS2 expression was found significantly increased in the inflamed relative to non-involved samples, although the effect sizes were small (Figure 2a, lower panels).

With IF microscopy (patient details in Table S2), we could not appreciate differences in ACE2 expression in the ileum, which possibly stemmed from the elevated physiological expression of ACE2. In the colon, patchy epithelial ACE2 expression from control non-IBD controls increased in IBD patients with inflammation and this increase was mostly evident on the crypt epithelium (Figure S2a).

In the ileum, low intensity TMPRSS2 expression on the crypt epithelium was also comparable in inflamed or uninflamed mucosal segments from IBD patients and in non-inflamed mucosal segments from non-IBD controls. In the colon, TMPRSS2 expression appeared comparable in IBD patients and non-IBD controls. In the rectum, TMPRSS2 expression was enhanced by inflammation (Figure S2a). Thus, colonic or rectal inflammation increases ACE2 and TMPRSS2 protein expression, respectively.

Age and gender but not smoking increases ACE2 mRNA in the healthy colon

In general, the ACE2 mRNA was higher with age in the uninflamed colonic samples. However, these effects were essentially nullified in the presence of inflammation. While age had no effect on TMPRSS2 mRNA levels in uninflamed GI tissues, a positive association with age in inflamed CD ileum and a negative association in inflamed UC colon biopsies was observed. ACE2 mRNA in the colon was significantly lower in males versus females but no gender associations in TMPRSS2 mRNA levels were found (Figure S2b-c). The expression of ACE2 and TMPRSS2 was similar when comparing active smokers to non-smokers, either between healthy controls or IBD patients (data not shown) and no significant interactions with inflammation status, region or other covariates were found. Thus, age and gender, but not smoking modulates ACE2 but not TMPRSS2 mRNA expression in the healthy colon.

Effect of non-biological medication (corticosteroids, thiopurines and 5-aminosalicylate) use on ACE2 and TMPRSS2 gene expression in the GI tract

We further evaluated the impact of non-biologic and biologic medication use (self-reported) on the expression of ACE2 and TMPRSS2 mRNA (Table S3) by propensity matching the MSCCR cohort (see supplementary methods).

In the *ileum* of IBD (CD) patients, corticosteroid, thiopurine or 5-aminosalicylate use had no impact on ACE2 mRNA expression in either inflamed or uninflamed biopsies (Figure 3a-c). In the *rectum*, however, a significant decrease in ACE2 mRNA expression was observed with corticosteroid use in inflamed biopsies. A similar decrease of ACE2 mRNA was noticed in thiopurine-treated non-inflamed samples. The use of corticosteroids, thiopurine or 5-aminosalicylate did not significantly affect TMPRSS2 mRNA expression in ileum samples. However, each of these three medications significantly decreased TMPRSS2 mRNA expression in inflamed rectum or colon samples. Thus, corticosteroid, thiopurine or 5-aminosalicylate attenuated ACE2 and TMPRSS2 mRNA expression in inflamed colon and rectum.

Effect of biologic medications (anti-TNF, vedolizumab and ustekinumab) on ACE2 and TMPRSS2 gene expression

We also defined the effect of current anti-TNF therapy (either adalimumab or infliximab) use on ACE2 and TMPRSS2 (Figure 3) expression. In the *ileum*, patients taking anti-TNF biologics did not show significantly different ACE2 or TMPRSS2 mRNA expression compared to those not on anti-TNF medication. In the large intestine, anti-TNF users showed increased ACE2 and TMPRSS expression, particularly in the inflamed rectum. Since the use cross-sectional cohort to study treatment effect has its limitations, we utilized published datasets from clinical trial cohorts, where longitudinal patient sampling was performed and information on endoscopic responses to treatment was available.

The results from a patient cohort treated with infliximab or vedolizumab on the GEMINI LTS trial[25] are summarized (Figure 4a-b) . Compared to baseline ACE2 expression, post-infliximab (week 6) colonic ACE2 gene expression was significantly lower and this decrease was observed predominantly in endoscopic responders (Figure 4b). In contrast, post-vedolizumab (week 6) ACE2 gene expression did not significantly change, although a nominally significant decrease was observed in endoscopic responders (Figure 4a-b). Finally, neither vedolizumab nor infliximab modified TMPRSS2 expression. These data suggest that resolution of inflammation decreases and potentially normalizes ACE2 expression in the inflamed colon.

To study the impact of IL-12/IL-23-targeting ustekinumab on ACE2 and TMPRSS2 mRNA levels in IBD, we used the CERTIFI trial cohort[24, 37]. We first confirmed that, as in our MSCCR cohort, ACE2 gene expression was indeed higher in uninflamed ileum compared to the colon regions (Figure S3a). Next, we observed that ileal ACE2 gene expression was significantly decreased with inflammation as was observed in the ileal samples from both MSCCR and RISK cohorts (Figure S3a). In colon and rectum samples, a trend to increase ACE2 expression in inflamed biopsies as compared with non-inflamed was also observed (Figure S3a).

Following ustekinumab treatment, ACE2 gene expression was increased (nominal significance) in the inflamed tissue (both small and large intestinal) after week 6 post ustekinumab as compared to the

screening biopsy (Figure 4c, Figure S3b) contrasting with a decrease in expression in placebo-treated patients. Upon examining expression by ustekinumab response at week 22, the increase of ACE2 and TMPRSS2 expression was mainly observed in the colon and was stronger in responders (fold-change=1.79, p=0.055 for ACE2 and fold-change= 2.25, p=0.024 for TMPRSS2). Thus, TNF-targeting biologics attenuated ACE2 mRNA expression in the inflamed colon, whereas IL-12/IL-23-targeting biologics increased both ACE2 and TMPRSS2 mRNA expression in the inflamed colon, particularly in therapy responders. A summary of the changes of examined clinical parameters and IBD medications on ACE2 and TMPRSS2 mRNA is in Figure S4.

Intestinal ACE2 gene regulatory subnetworks are enriched in metabolic functions and interferon signaling in the inflamed colon

To identify potential functions associated with ACE2 and TMPRSS2 in the gut, we studied these genes in the context of Bayesian regulatory gene networks (BGRNs). These probabilistic graphical models consider all available trait data (gene expression and genotype) simultaneously in order to derive gene:gene casual relationships amongst thousands of intermediate molecular traits[38].

The nearest neighbors of ACE2 were extracted including genes within either 3 to 5 path lengths in each BGRN network (5 networks total) keeping the subnetwork sizes relatively similar (~200-300 genes, Figure 5a-5d, Table S7). Immediate neighbors of ACE2 in the ileum CD network included SLC6A19 (a known interacting partner of ACE2[39]), and other SLC transporters but also other viral-associated receptor proteins, like DPP4 and EZR[40]. A summary of the recurring genes across subnetworks is shown (Figure 5b-5e).

Each ACE2-associated subnetwork was interrogated for functional enrichment in the ileum (Figure 5c) or colon (Figure 5f) using the Reactome database and included metabolic pathways such as SLC-mediated transport; xenobiotic metabolism; vitamins and cofactors; and hexose transport. Additional ileum-associated pathways included amino acid and oligopeptide SLC transporters, while colon-associated networks included interferon and immune signaling.

Next, we compared the ACE2-associated subnetworks to a single-cell transcriptomic study of IBD patients using the top 300 genes (ranked by p value) reported to be correlated with ACE2 expression in colonocytes[35]. Consistent with the origin of the ACE2-correlated geneset, we observed significant enrichment mainly in the ACE2-associated colonic BGRN subnetworks (Figure S5a), thereby supporting our approaches. Thus our ACE2-subnetworks are a novel source of insight into the regulation and function of ACE2.

We further evaluated the enrichment of genesets marking distinct intestinal cell types derived from single cell data[32, 33] on ACE2- subnetworks and observed significant enrichment mainly epithelial cell types,

including enterocytes and absorptive cells (Figure S5b-c). In the colon, ACE2-associated subnetworks from IBD patients showed co-enrichment in immune cell types, namely myeloid macrophages, Treg and MAIT cells, as well as gene signatures derived from macrophages following various cytokine perturbations including IFNg/b[34] (Figure S5c-d). Thus, the gut ACE2 gene regulatory sub-networks are co-enriched in gene sets from epithelial and immune cells, particularly in the inflamed colon and predominantly reveal metabolic functions and innate immune processes, including type-1 interferon signaling in the inflamed colon.

Intestinal TMPRSS2 gene regulatory subnetworks are predominantly enriched for metabolic functions

To address the function of TMRPSS2, the subnetworks associated with TMPRSS2 were extracted from the BGRNs (Figure S6a) allowing three or four layers to obtain similar subnetworks sizes (~200–300 genes). TMPRSS2 was not found in the BGRN from the ileum of controls, likely due to low expression variance, a filter used before BGRN network construction (Table S13). Genes recurring in 4 of 4 subnetworks were identified (Figure S6b). TMPRSS2-associated subnetwork genes are enriched for cell-cell communication, tight junction interaction, O-linked glycosylation of mucins and membrane trafficking-associated pathways (Figure S6c). Consistent with these functions we observed enrichment of the TMPRSS2 subnetworks in genesets associated with enterocytes, goblet and secretory cells (Figure S7 a-b).

Expression of SARS-CoV2 responsive genes in lung cells is generally higher with IBD inflammation

To understand the impact of IBD-driven gut inflammation on the pathogenesis of COVID-19, we examined a host molecular response signature generated following SARS-CoV-2 infection of a primary human lung epithelium (NHBE) cell and a transformed lung alveolar cell line (A549)[27]. Using GSVA, we generated a single score summarizing expression of either up or down-regulated COVID-19-responsive genes, according to intestinal region, disease and inflammation status (Figure 6a-b). In general, the expression of genes up-regulated by SARS-CoV-2 infection was higher in inflamed regions as compared to uninflamed regions or non-IBD control subjects. We also confirmed this observation in the CERTIFI CD cohort (Figure S8a). We directly compared the genes associated with response to lung cell SARS-CoV2 infection and various IBD-centric genesets generated in our MSCCR cohort[41] or IBD GWAS genes. We observed that genes: up-regulated with inflammation, or positively associated with macroscopic or microscopic measures of disease, or associated with the risk of IBD, were enriched in genes up-regulated by SARS-CoV2 infection of lung epithelial cells (Figure S8b)

Taken together, these data support a congruence of molecular responses between IBD-associated enteric inflammation and epithelial infection by SARS-CoV-2. such that COVID-19 and IBD disease outcomes may be reciprocally influenced.

IBD inflammation and COVID-19 response gene subnetworks converge at molecular pathways linked to IFN and IL-6

To interrogate the potential intersection of SARS-CoV-2 infection and IBD inflammatory responses, we generated NHBE-COVID-19 associated subnetworks (NHBE-COVID_subnet) and IBD inflammation associated subnetworks (IBD_Inf_subnet) from three IBD BGRNs (Table S17). We then determined the overlap between them, with the rationale that common gene membership implies similar molecular pathobiologies. We observed a significant overlap between IBD-Inf and NHBE-COVID_subnets across all three independent networks tested (Figure 6c). We also noted that the intersecting genes (148 in ileum CD, 213 in Colon UC and 170 in Colon CD networks) were enriched in candidate IBD GWAS genes (Table S18).

To determine the underlying shared pathobioological mechanisms we evaluated enrichment of the three *intersecting* subnetworks against Reactome pathways. The majority of the pathways were immune oriented with the most striking related to innate immune signaling via interferon and interleukin-6 (Figure 6d, Table S19). This finding is consistent with a large body of recent data that describe a dramatic up-regulation of pro-inflammatory cytokines in patients with COVID-19[8] including induction of IFN-stimulated genes[27].

We confirmed these observation using the recent dataset wherein hSIOs were infected with SARS-CoV-2[28]. hSIOs were grown in either Wnt high EXP medium and consist mainly of stem cells and enterocyte progenitors or a DIF medium and consist of enterocytes, goblet cells and some enteroendocrine cells. GSVA analysis confirmed that inflamed MSCCR biopsies had higher expression of genes found altered in hSIOs following SARS-CoV-2 infection. (Figure S9a-b). Direct overlap of genesets from the hSIO-COVID-19 models and various IBD-centric genesets showed similar enrichments as with the lung-COVID-19 model (Figure S9c). Finally, subnetworks generated in the ileum CD using hSIO-COVID-19 responsive genesets (Table S20) intersected with IBD-Inf associated subnetworks. The intersecting genes were similar to those found between IBD-Inf and NHBE-COVID19-associated ileum CD subnetworks, containing many interferon-stimulated genes (Figure S9d-e). This further emphasizes a shared molecular pathology between COVID-19 response and IBD inflammation.

Identification of key driver genes (KDGs) at the intersection of IBD and COVID-19

As a data reduction approach, we evaluated the NHBE-COVID-19 and IBD-Inflammation molecular response subnetworks for KDGs. We summarized the top recurring KDGs shared by IBD inflammation and NHBE-COVID-19 molecular responses across the three BGRNs (Figure 6e, Table S21). Included were interferon-stimulated genes such as IRF1, GBP1/2, PARP14/9 and several of these were replicated in BGRNs from the RISK and CERTIFI cohort including CXCL1, GBP4, PARP9 amongst others (data not shown).

Genes overlapping between IBD inflammation and COVID-19 infection are enriched in subnetworks associated with response to IBD therapy

Finally, in patients with Ileal CD, we generated subnetworks associated with response to infliximab or ustekinumab (Table S22). We then tested their enrichment in the subnetworks associated with individual COVID-19 infection models (lung and hSIOs) or a common COVID-19 associated subnetwork using genes which were commonly up-regulated in both systems. We observed significant intersections between genes associated with IBD therapy and either IBD-inflammation or COVID-infection (Table S23, Figure 6f) indicative of commonality between COVID-19 and response to IBD treatment.

Discussion

The objective of this study was to systematically determine the molecular intersections between COVID-19-associated inflammation, IBD and immunomodulatory drugs. Our data provides mRNA- and protein-level evidence of the regional distribution of ACE2 and TMPRSS2 across different parts of the GI tract and the impact of the commonly used IBD medications on ACE2 and TMPRSS2 expression in the inflamed and uninflamed intestines. Furthermore, utilizing BGRNs, we provide novel intestinal gene:regulatory relationships for ACE2 and TMPRSS2 and demonstrate commonality between molecular subnetworks underlying IBD-associated intestinal inflammation and SARS-CoV-2-associated epithelial infection. Finally, we observe that this common molecular signal partially overlaps with molecular subnetworks containing anti-TNF and anti-IL 12/23 response-associated genes.

ACE2 has a less appreciated RAS-independent role in the intestine by promoting amino acid absorption. Consistent with this function we observed high levels of ACE2 expression in the small bowel brush border[42-44] supportive of the role of ACE2 in mucosal homeostasis[43]. Remarkably, the analyses of gene:regulatory networks empirically derived from the terminal ileum, showed that ACE2 was co-regulated with SLC6A19, an amino acid transporter that physically interacts with ACE2[45]. The colon BGRN derived ACE2 subnetwork would also suggest, a potential metabolic role for ACE2 in the colon including solute carrier dependent processes.

TMPRSS2 is expressed in multiple tissues including the prostate, breast, biliary epithelium, kidney, salivary glands, stomach, colon, small intestines and lung[46-48]. While the physiological function of TMPRSS2 remains largely elusive, it has been linked to epithelial sodium channel (ENaC) regulation[49] and possibly in regulating sperm function[50]. In agreement with literature[49], our BGRN analysis showed SCNN1A, which corresponds to a subunit of the ENaC, associated with TMPRSS2. Remarkably, gene products co-localized with TMPRSS2 were consistently enriched in fundamental epithelial functions. For example, F11R, which encodes a JAM-A protein mediates tight junction formation. Interestingly, we noted connections to viral responses. JAM-A is a reovirus receptor[51] and TRIM31[52] and BAIAIP2L1[53] associate with mitochondrial anti-viral associated proteins.

We hypothesize that the upper GI tract may be involved in SARS-CoV-2 entry and intestinal epithelial cells may augment the replication of SARS-CoV-2 and contribute to viral dissemination. 2-50% of COVID19 patients have specific GI symptoms often preceding respiratory symptoms[5, 35, 54-57]. Therefore, we need to understand the intersections between COVID and known GI disorders such as IBD[18, 19, 58, 59]. We have observed a reduction in ACE2 expression in the inflamed ileum and smaller increase in the inflamed rectum**.** Since ACE2 appears to be a brush-border enzyme, its reduction with inflammation in the ileum is consistent with loss of expression of other brush border enzymes during enteritis[60]. That said, even during inflammation, the expression of ACE2 remains significant in the small intestines.

The major classes of IBD medications do not appear to have a major impact on ileal gene expression of ACE2 or TMPRSS2 (Figure S4). In contrast, their effect appears to be mediated through the resolution of gut inflammation. This is biologically plausible since none of the drugs used in IBD therapeutics are directed at the intestinal epithelium, the site of expression of ACE2 and TMPRSS2. These data are further supported by real-time data from a registry of IBD-COVID patients wherein we did not find a significant association between anti-TNF use and the risk of severe COVID-19 disease[59].

Given that COVID-19 and IBD are inflammatory pathologies, we posit that selected IBD therapies may potentially be useful in treating the inflammatory aspects of COVID-19. First we observed higher expression of SARS-CoV-2 lung cell infection genes in inflamed gut biopsies (ileum and colon) than non-inflamed tissues. Secondly, by integrating a lung cell COVID-19 molecular response signature with intestinal BGRNs we show a common subnetwork between the response to SARS-CoV-2- and IBD-associated gut inflammation. The intersecting biology was enriched in IBD susceptibility genes, partially overlapped IBD drug responsive subnetworks and revealed interferon and IL-6 signaling to be at the point of intersection. Our network analysis also supports the fact that the cytokine profile of patients with severe COVID-19 infection resembles that seen in the inflamed intestine of IBD patients. As such targeting of ongoing mucosal inflammation in IBD may ultimately be beneficial[21]. Clinical trials using IL-6 blockade in COVID-19 are currently underway. Other potential targets suggested in our analysis include KDGs such

as PARP9 and PARP14. PARP14, a mono-ADP ribosylation enzyme is particularly interesting, given that related coronaviruses encode a macrodomain to reverse ADP-ribosylation, which facilitates viral replication and virulence[61]. A recent study suggests repurposing of PARP1 inhibitors for therapeutic targeting of COVID-19[62].

In summary, through detailed analyses of intestinal tissues in health and IBD, we conclude that the expression of ACE2 and TMPRSS2 supports local, GI-associated replication of SARS-COV-2. Whether or not infectious virions can be transmitted early in disease course remains a high priority investigation. Further, a majority of the frontline IBD medications do not appear to alter ACE2 or TMPRSS2 expression to a significant degree, supporting a rationale for the continued use of these agents in clinically indicated conditions. In contrast, there are certain molecular responses that appear in common between SARS-COV-2 and IBD inflammation which may suggest potential new avenues for COVID-19 treatment.

Key words: SARS-CoV-2, COVID-19, GI tract, ACE2, TMPRSS2, network analyses, IBD medications.

Figure Legends:

Figure 1. Robust ACE2 expression is found on small bowel surface epithelium in both children and adults. Representative immunofluorescence images of ACE2 (green) and EPCAM (red) counterstained with DAPI (blue) in intestinal biopsies of healthy patients, including magnified images of surface epithelium (se) and crypt epithelium (ce). **A.** Duodenal biopsies, **B.** Terminal ileum biopsies (Goblet cell indicated with arrows. and **C. Colonic** biopsies. Patient age (years) and sex (M, male; F, female) as indicated. Isotype controls and no primary controls for each segment are included on the far right of each panel. Scale bar, 100µm.

Figure 2: Expression of ACE2 and TMPRSS2 in intestinal biopsies of adult and pediatric IBD patients and controls. A. Box plot summarizing the normalized expression level of ACE2 (upper panel) and TMPRSS2 (lower panel) as measured in ileum or colonic and rectal biopsies from control and IBD MSCCR patients, which were either endoscopically inflamed (IBD.I) or non-inflamed (Non.I). **B**. Box plot summarizing the normalized expression level of ACE2 (left panel) and TMPRSS2 (right panel) as measured in ileum CD samples from the RISK pediatric cohort. Clinical characteristics of MSCCR IBD patients and biopsies are summarized in Table S3 and S4.

Figure 3: The effect of IBD medication use on expression of ACE2 and TMPRSS2 in intestinal biopsies of IBD and control MSCCR patients. Propensity-matched cohorts of UC and CD MSCCR patients receiving or not receiving corticosteroids (**A**); thiopurines (**B**); 5-aminosalicylates (**C**); or anti-TNF (**D**) were used to estimate the mean (+-SEM) differences in ACE2 (upper panel) and TMPRSS2 (lower panel) expression between the medicated and non-medicated groups. P-values <0.1 are reported. Under the model, we estimated the change in ACE2 or TMPRSS2 gene expression between the medicated and non-medicated group according to disease subtype (CD, UC) region (ileum, colon, rectum) and tissue type (inflamed, non-inflamed). Samples sizes are in Table S5.

Figure 4: The effect of ustekinumab and vedolizumab on ACE2 and TMPRSS2 expression. A-B) Changes on colonic gene expression profiles for ACE2 (upper panel) and TMPRSS2 (lower panel) on patients treated with vedolizumab (VDZ) or infliximab (IFX). **A**.) Estimated marginal means for the expression (M+-SEM) at baseline and week 4-6. **B**.) Differences in endoscopic responders and non-responders at week 4-6 versus baseline samples. **C-D.**) Changes in gut expression of ACE2 (upper panel) and TMPRSS2 (lower panel) in CD patients treated with ustekinumab (CERTIFI cohort). **C**). Estimated marginal means for the expression (M+-SEM) at baseline and week 6 for inflamed and non-inflamed biopsies. **D.**) As no change was observed in non-inflamed biopsies, treatment effect on inflamed biopsies

was compared between week-22 clinical responders and non-responders versus baseline. P-values denote significance of each time point compared to screening visit +(P<0.1), *(P<0.05), **(P<0.01). Samples sizes are in Table S6.

Figure 5: BGRN analysis of ACE2 reveals metabolic function and interferon pathway associations. The ACE2 associated subnetworks extracted from the (**A**.) Ileum CD BGRN (235 of 8458 nodes total) or from the (**D**) Colon CD BGRN (235 of 8549 total nodes). Genes (nodes) found within the first, second or third/fourth layer are colored blue, yellow or grey, respectively. Five ACE associated subnetworks were generated (Table S7). **B**. and **E**. A summary of the genes found in both ileum and colon ACE2-associated networks. Subnetwork sizes are: Control_ileum = 221; CD_ileum= 235; Control_colon = 229; CD_colon = 235 and UC_colon = 346. **C** and **F** Reactome pathway enrichment analysis of ACE2-associated subnetworks (with BH adj P <0.1). The heatmap depicts fold enrichment. Level of significance is indicated by either *, ** or *** for p-value of >0.1, >0.05 or >0.01, respectively (Table S8 for full results).

Figure 6: Molecular genes associated with IBD inflammation overlap with genes responsive to COVID-19 infection in lung cells. A. We evaluated expression of COVID-19-responsive genes as determined in NHBE (A) or A549 (B) lung epithelial cell models[27] in the MSCCR biopsy samples using GSVA. Mixed linear modeling (gene~region*tissue type) was performed to compare expression between control, non-inflamed and inflamed samples and the box plots summarize the mean expression (+/- SEM) of the two signatures (Sample sizes in Table S4, *** indicates p value <0.001). **C**. Three NHBE-COVID-19-and three IBD-Inf- associated subnetworks, one each for ileum CD, colon UC and colon CD BGRNs were generated (Table S17 and S18). Venn diagrams of the overlap in subnetwork genes including the fold enrichment (FE) and a p-value of the enrichment test. **D**. The 3 intersecting genesets were interrogated for enrichment in the Reactome database. Heatmap depicting the FE in pathways (BH adj p<0.1 and minimum 5-fold enrichment, Table S19). **E**. KDGs were determined, separately, for NHBE-COVID-19 or IBD-Inf signature genes in each BGRN and a summary of the top recurring KDGs presented (Table S21). A gene was considered a KDG if its subnetwork (within 3 layers) was significantly enriched (Adj p<0.05) in signature genes. **F**. Subnetworks were generated from CD Ileum BGRNs associated with either: 1. IBD-inflammation genes; 2. COVID-19 responsive genes derived from each of the lung or hSIO models or a common COVID-19-molecular response signature derived from intersecting the models[27, 28]; and 3. Infliximab or ustekinumab drug response ileal signatures. Results of enrichment of drug response subnetworks in either IBD-inflammation or COVID-19 associated subnetworks (Table S22/23 for results) are shown.

References:

1. Gorbalenya AE, Baker SC, Baric RS, et al. The species Severe acute respiratory syndrome-related coronavirus: classifying 2019-nCoV and naming it SARS-CoV-2. Nature Microbiology 2020;5:536-544.
2. Coronavirus disease 2019 (COVID-19) Situation Report – 51: World Health Organization.
3. Coronavirus Disease 2019 (COVID-19):Symptoms of Coronavirus: Centers for Disease Control and Prevention, 2020.
4. Zhang H, Kang Z, Gong H, et al. The digestive system is a potential route of 2019-nCov infection: a bioinformatics analysis based on single-cell transcriptomes. bioRxiv 2020.
5. Jin X, Lian J-S, Hu J-H, et al. Epidemiological, clinical and virological characteristics of 74 cases of coronavirus-infected disease 2019 (COVID-19) with gastrointestinal symptoms. Gut 2020.
6. Tian Y, Rong L, Nian W, et al. Review article: gastrointestinal features in COVID-19 and the possibility of faecal transmission. Alimentary Pharmacology & Therapeutics 2020;51:843-851.
7. Pan L, Mu M, Ren HG, et al. Clinical characteristics of COVID-19 patients with digestive symptoms in Hubei, China: a descriptive, cross-sectional, multicenter study. Am J Gastroenterol 2020;20.
8. Huang C, Wang Y, Li X, et al. Clinical features of patients infected with 2019 novel coronavirus in Wuhan, China. Lancet 2020;395:497-506.
9. Giamarellos-Bourboulis EJ, Netea MG, Rovina N, et al. Complex Immune Dysregulation in COVID-19 Patients with Severe Respiratory Failure. Cell Host Microbe 2020.
10. Turner AJ, Tipnis SR, Guy JL, et al. ACEH/ACE2 is a novel mammalian metallocarboxypeptidase and a homologue of angiotensin-converting enzyme insensitive to ACE inhibitors. Canadian Journal of Physiology and Pharmacology 2002;80:346-353.
11. Donoghue M, Hsieh F, Baronas E, et al. A novel angiotensin-converting enzyme-related carboxypeptidase (ACE2) converts angiotensin I to angiotensin 1-9. Circulation research 2000.
12. Vickers C, Hales P, Kaushik V, et al. Hydrolysis of biological peptides by human angiotensin-converting enzyme-related carboxypeptidase. Journal of Biological Chemistry 2002.
13. Rabelo LA, Alenina N, Bader M. ACE2–angiotensin-(1–7)–Mas axis and oxidative stress in cardiovascular disease. Hypertension Research 2011;34:154-160.
14. Hoffmann M, Kleine-Weber H, Schroeder S, et al. SARS-CoV-2 Cell Entry Depends on ACE2 and TMPRSS2 and Is Blocked by a Clinically Proven Protease Inhibitor. Cell 2020.
15. Guo Y-R, Cao Q-D, Hong Z-S, et al. The origin, transmission and clinical therapies on coronavirus disease 2019 (COVID-19) outbreak – an update on the status. Military Medical Research 2020.
16. Xu X, Chen P, Wang J, et al. Evolution of the novel coronavirus from the ongoing Wuhan outbreak and modeling of its spike protein for risk of human transmission. Science China Life Sciences 2020;63:457-460.
17. Gurwitz D. Angiotensin receptor blockers as tentative SARS-CoV-2 therapeutics. Drug Development Research 2020.

18. Torres J, Mehandru S, Colombel J-F, et al. Crohn's disease. The Lancet 2017;389:1741-1755.
19. Ungaro R, Mehandru S, Allen PB, et al. Ulcerative colitis. The Lancet 2017;389:1756-1770.
20. Danese S, Cecconi M, Spinelli A. Management of IBD during the COVID-19 outbreak: resetting clinical priorities. Nature Reviews Gastroenterology & Hepatology 2020.
21. Monteleone G, Ardizzone S. Are Patients with Inflammatory Bowel Disease at Increased Risk for Covid-19 Infection? Journal of Crohn's and Colitis 2020.
22. de Lang A, Osterhaus ADME, Haagmans BL. Interferon-γ and interleukin-4 downregulate expression of the SARS coronavirus receptor ACE2 in Vero E6 cells. Virology 2006;353:474-481.
23. Haberman Y, Tickle TL, Dexheimer PJ, et al. Pediatric Crohn disease patients exhibit specific ileal transcriptome and microbiome signature. The Journal of Clinical Investigation 2014;124:3617-3633.
24. Peters LA, Perrigoue J, Mortha A, et al. A functional genomics predictive network model identifies regulators of inflammatory bowel disease. Nature Genetics 2017;49:1437-1449.
25. Arijs I, De Hertogh G, Lemmens B, et al. Effect of vedolizumab (anti-α4β7-integrin) therapy on histological healing and mucosal gene expression in patients with UC. Gut 2018;67:43.
26. Shannon P, Markiel A, Ozier O, et al. Cytoscape: a software environment for integrated models of biomolecular interaction networks. Genome research 2003;13:2498-2504.
27. Blanco-Melo D, Nilsson-Payant BE, Liu W-C, et al. SARS-CoV-2 launches a unique transcriptional signature from in vitro, ex vivo, and in vivo systems. bioRxiv 2020:2020.03.24.004655.
28. Lamers MM, Beumer J, van der Vaart J, et al. SARS-CoV-2 Productively Infects Human Gut Enterocytes. bioRxiv 2020:2020.04.25.060350.
29. Arijs I, De Hertogh G, Lemaire K, et al. Mucosal gene expression of antimicrobial peptides in inflammatory bowel disease before and after first infliximab treatment. PLoS One 2009;4:e7984.
30. VanDussen KL, Stojmirovic A, Li K, et al. Abnormal Small Intestinal Epithelial Microvilli in Patients With Crohn's Disease. Gastroenterology 2018;155:815-828.
31. Kuleshov MV, Jones MR, Rouillard AD, et al. Enrichr: a comprehensive gene set enrichment analysis web server 2016 update. Nucleic acids research 2016;44:W90-W97.
32. Smillie CS, Biton M, Ordovas-Montanes J, et al. Intra- and Inter-cellular Rewiring of the Human Colon during Ulcerative Colitis. Cell 2019;178:714-730.e22.
33. Huang B, Chen Z, Geng L, et al. Mucosal Profiling of Pediatric-Onset Colitis and IBD Reveals Common Pathogenics and Therapeutic Pathways. Cell 2019;179:1160-1176.e24.
34. Xue J, Schmidt SV, Sander J, et al. Transcriptome-based network analysis reveals a spectrum model of human macrophage activation. Immunity 2014;40:274-288.
35. Wang J, Zhao S, Liu M, et al. ACE2 expression by colonic epithelial cells is associated with viral infection, immunity and energy metabolism. medRxiv 2020:2020.02.05.20020545.
36. Zhang B, Zhu J. Identification of Key Causal Regulators in Gene Networks. Lecture Notes in Engineering and Computer Science 2013;2:1309-1312.

37. Sandborn WJ, Gasink C, Gao L-L, et al. Ustekinumab Induction and Maintenance Therapy in Refractory Crohn's Disease. New England Journal of Medicine 2012;367:1519-1528.
38. Schadt EE, Lamb J, Yang X, et al. An integrative genomics approach to infer causal associations between gene expression and disease. Nature Genetics 2005;37:710-717.
39. Camargo SMR, Singer D, Makrides V, et al. Tissue-Specific Amino Acid Transporter Partners ACE2 and Collectrin Differentially Interact With Hartnup Mutations. Gastroenterology 2009.
40. Millet JK, Kien F, Cheung C-Y, et al. Ezrin Interacts with the SARS Coronavirus Spike Protein and Restrains Infection at the Entry Stage. PLOS ONE 2012;7:e49566.
41. Huang R, Irizar H, Kosoy R, et al. OP17 A molecular measure of inflammation in IBD patients based on transcriptional profiles from 2495 intestinal biopsies. Journal of Crohn's and Colitis 2019;13:S011-S012.
42. Hamming I, Timens W, Bulthuis MLC, et al. Tissue distribution of ACE2 protein, the functional receptor for SARS coronavirus. A first step in understanding SARS pathogenesis. Journal of Pathology 2004.
43. Hashimoto T, Perlot T, Rehman A, et al. ACE2 links amino acid malnutrition to microbial ecology and intestinal inflammation. Nature 2012;487:477-81.
44. Bai JP. Distribution of brush-border membrane peptidases along the rat intestine. Pharm Res 1994;11:897-900.
45. Kowalczuk S, Broer A, Tietze N, et al. A protein complex in the brush-border membrane explains a Hartnup disorder allele. FASEB J 2008;22:2880-7.
46. Jacquinet E, Rao NV, Rao GV, et al. Cloning, genomic organization, chromosomal assignment and expression of a novel mosaic serine proteinase: epitheliasin. FEBS Lett 2000;468:93-100.
47. Lin B, Ferguson C, White JT, et al. Prostate-localized and androgen-regulated expression of the membrane-bound serine protease TMPRSS2. Cancer Res 1999;59:4180-4.
48. Lucas JM, True L, Hawley S, et al. The androgen-regulated type II serine protease TMPRSS2 is differentially expressed and mislocalized in prostate adenocarcinoma. The Journal of Pathology 2008;215:118-125.
49. Gaillard EA, Kota P, Gentzsch M, et al. Regulation of the epithelial Na+ channel and airway surface liquid volume by serine proteases. Pflugers Arch 2010;460:1-17.
50. Chen YW, Lee MS, Lucht A, et al. TMPRSS2, a serine protease expressed in the prostate on the apical surface of luminal epithelial cells and released into semen in prostasomes, is misregulated in prostate cancer cells. Am J Pathol 2010;176:2986-96.
51. Lai CM, Boehme KW, Pruijssers AJ, et al. Endothelial JAM-A promotes reovirus viremia and bloodstream dissemination. The Journal of infectious diseases 2015;211:383-393.
52. Liu B, Zhang M, Chu H, et al. The ubiquitin E3 ligase TRIM31 promotes aggregation and activation of the signaling adaptor MAVS through Lys63-linked polyubiquitination. Nature Immunology 2017;18:214-224.
53. Xia P, Wang S, Xiong Z, et al. IRTKS negatively regulates antiviral immunity through PCBP2 sumoylation-mediated MAVS degradation. Nature Communications 2015;6:8132.

54. Wang D, Hu B, Hu C, et al. Clinical Characteristics of 138 Hospitalized Patients With 2019 Novel Coronavirus–Infected Pneumonia in Wuhan, China. JAMA 2020;323:1061-1069.
55. Ma FH, Hu HT, Tian YT. [Surgical treatment strategy for digestive system malignancies during the outbreak of novel coronavirus pneumonia]. Zhonghua zhong liu za zhi [Chinese journal of oncology] 2020;42:E001.
56. Sultan S, Lim JK, Altayar O, et al. AGA Institute Rapid Recommendations for Gastrointestinal Procedures During the COVID-19 Pandemic. Gastroenterology 2020.
57. Chen N, Zhou M, Dong X, et al. Epidemiological and clinical characteristics of 99 cases of 2019 novel coronavirus pneumonia in Wuhan, China: a descriptive study. The Lancet 2020;395:507-513.
58. Ng SC, Shi HY, Hamidi N, et al. Worldwide incidence and prevalence of inflammatory bowel disease in the 21st century: a systematic review of population-based studies. The Lancet 2017;390:2769-2778.
59. Brenner EJU, R.C.; Colombel, J.F.; Kappelman, MD. . SECURE-IBD Database Public Data Update, 2020.
60. Bailey DS, Freedman AR, Price SC, et al. Early biochemical responses of the small intestine of coeliac patients to wheat gluten. Gut 1989;30:78-85.
61. Grunewald ME, Chen Y, Kuny C, et al. The coronavirus macrodomain is required to prevent PARP-mediated inhibition of virus replication and enhancement of IFN expression. PLoS Pathog 2019;15:e1007756.
62. Ge Y, Tian T, Huang S, et al. A data-driven drug repositioning framework discovered a potential therapeutic agent targeting COVID-19. bioRxiv 2020:2020.03.11.986836.

ACKNOWLEDGMENTS

We thank the patients who participated in the study.

Funding: This work was supported by the following grants: NIH/NIDDK R01 112296 (SM). Additional support was provided by K23KD111995 (RCU) and a Career Development Award from the Crohn's and Colitis Foundation (RCU). CA, MSF were supported by a Litwin Pioneers award grant. CA and ES were supported in part by the the Helmsley Charitable Trust. MT was supported by the Digestive Disease Research Foundation (DDRF). The sampling of the Inflammatory Bowel Disease cohort (Crohn's disease and ulcerative colitis) was jointly designed as part of the research alliance between Janssen Biotech, Inc. and The Icahn School of Medicine at Mount Sinai. Beyond this exception, no other funders had a role in analyses design and interpretation. This work was supported in part through the computational resources and staff expertise provided by Scientific Computing at the Icahn School of Medicine at Mount Sinai.

Supplementary Legends:

Figure S1. TMPRSS2 and ACE2 distribution and localization in the intestine. Representative immunofluorescence images of ACE2 (green) and TMPRSS2 (red) counterstained with DAPI (blue) in intestinal biopsies of non-IBD patients. Magnified images of surface epithelium (se) and crypt epithelium (ce) showing only TMPRSS2 and DAPI. **a,** Duodenal biopsies from pediatric and adult patients **b**, Terminal ileum biopsies from adult patients. **c**, Biopsies from indicated colonic segments in adult patients. Patient age (years) and sex (M, male; F, female) indicated in the top left corner of each image. Isotype controls and no primary controls for each segment are included on the far right of each panel. Scale bar, 100µm.

Figure S2: Expression of ACE2 and TMPRSS2 protein and summary of the effects of age and gender on ACE2 and TMPRSS2 gene expression in the intestine. A. Representative immunofluorescence images of ACE2 (green) and DAPI (blue) on the left and TMPRSS2 (red) and DAPI (blue) on the right in paired inflamed and uninflamed IBD intestinal specimens. Terminal ileum from a CD patient pre-IFX (inflamed) and after IFX treatment (uninflamed). Inflamed left colon and uninflamed sigmoid colon from a UC patient pre-biologic. Inflamed rectum from a CD patient pre- IFX and uninflamed rectum post-IFX therapy. Clinical characteristics of IBD patients and biopsies are summarized in supplemental table 3. **B.** Age effect (coefficient) was calculated for CD and UC at different regions (Ileum and Colon). P values denote significance of effect of age on gene expression at a disease and tissue group, +(P<0.1), *(P<0.05), **(P<0.01). **C**. We estimated the marginal mean expression of ACE2 and TMPRSS2 for male and female at each region (Ileum and Colon) and disease (CD and UC) group. P values highlighted if significant difference between males and females was found.

Figure S3: The effect of ustekinumab (CERTIFI cohort) by region on ACE2 and TMPRSS2 gene expression in the intestine. A. we estimated the marginal mean expression of ACE2 and TMPRSS2 at baseline Inflamed and Non-inflamed tissue and across different regions (Ileum, Colon and Rectum). P values indicated the significance of comparisons between tissue type (Inflamed vs. Non-Inflamed). On average, the expression level of ACE2 was higher at Ileum than at other regions. Within Ileum, significant difference was found between the inflamed and non-inflamed tissue. The expression level of TMPRSS2 was lower at Ileum than at other regions. Only at colon, we were able to detect significant differences between inflamed and non-inflamed tissues. **B.** The marginal mean expressions of ACE2 and TMPRSS2 were estimated for ustekinumab and placebo group at baseline and week 6 across different regions. P values denote significance of change at Week 6 from screening, +(P<0.1), *(P<0.05), **(P<0.01). Expression level

of ACE increased at ustekinumab group at all regions, however, no significance was found. There is a significant increase of TMPRSS2 at inflamed colon at week 6 from screening. The samples sizes are summarized in Table S6.

Figure S4: Summary of the effects of demographics, age, gender, inflammation and medication use on ACE2 and TMPRSS2 gene expression in the intestine. Arrows are used to indicate the effect of various conditions on ACE2 or TMPRSS2 gene expression in the ileum or large intestine (colon or rectum). Lighter colored arrows represent nominal significance (p between 0.1 and 0.05) and darker arrows represent significance of $p<0.05$ in the various contrasts listed. Whether the effect is found in inflamed (Inf) or non-inflamed (Non.I) biopsies is indicated.

Figure S5: ACE2 associated subnetworks reveals gut epithelial cell type enrichment. Each ACE2 associated subnetwork was interrogated for enrichment with: **A.** Genes co-correlated with ACE2 in colonocytes was curated from Wang et al[35]; Gut cell type associated signatures from (Huang et al.,2019[33]) (**B**) and (Smillie et al., 2019[32]) (**C**); **D**. Gene sets associated with various perturbations in macrophages[34]. The number of genes within each ACE2 associated subnetwork are: Control ileum = 221; CD ileum= 235; Control colon = 229; CD colon = 235 and UC colon = 346. The heatmap colouring depicts the fold enrichment and the level of significance is indicated by either *, ** or *** for BH adj p value of either >0.1, >0.05 or >0.01, respectively. The full enrichment results are available in Tables S9 to S12.

Figure S6: Bayesian gene regulatory network (BGRN) analysis of TMPRSS2 reveals gut barrier function pathway associations. A. The TMPRSS2 subnetwork extracted from the Colon UC BGRN (490 of 8557 nodes total) was generated by including 4 additional layers of genes (undirected network expansion). Genes or nodes found within the first, second or third/fourth layer are colored blue, yellow or grey, respectively. In total 4 TMPRSS2 subnetworks were generated, one from ileum gene expression data from MSCCR CD patients and 3 from colon (and rectum) gene expression data from MSCCR control, UC, or CD patients (See Table S13). Both inflamed and non-inflamed biopsies were used for the IBD networks are shown. **B.** A summary of the genes found in 4 out of the 4 TMPRSS2 associated networks. The number of genes within each TMPRSS2 associated subnetworks are: CD ileum= 397; Control colon= 268; CD colon = 366 and UC colon= 490. **C**. Pathway enrichment analysis (Fisher's exact test) of each TMPRSS2 associated subnetwork according to Reactome pathways was performed. Only pathways which were found significantly enriched in at least one TMPRSS2 associated subnetwork (at BH adj P <0.1) are presented in the heatmaps in C. The heatmap coloring depicts the fold enrichment and the level of significance is

indicated by either *, ** or *** for BH adj p value of either >0.1, >0.05 or >0.01, respectively. The full enrichment results are available in Table S14.

Figure S7: TMPRSS2 associated subnetworks reveals gut cell type enrichment. Each of the four TMPRSS2 associated subnetworks were examined for enrichment with various gut cell type related signatures[32, 33] (Smillie et al.,2019) (**A**) (Huang et al., 2019) **B**. The number of genes within each TMPRSS2 associated subnetworks are: CD ileum= 397; Control colon= 268; CD colon = 366 and UC colon= 490. The heatmap coloring depicts the fold enrichment and the level of significance is indicated by either *, ** or *** for BH adj p value of either >0.1, >0.05 or >0.01, respectively. The full enrichment results are available in Tables S15 and S16.

Figure S8: Geneset variance analysis of COVID-19 responsive genes as determined in CERTIFI cohort gut biopsies. **A**. Two molecular expression signatures reflecting a host's transcriptional response to SARS-CoV-2 infection were curated from Blanco-Melo et al[27]. (Left panel) Transformed lung alveolar cell line (A549) and (Right panel) Primary human lung epithelium (NHBE) were profiled following SARS-CoV-2 exposure. We determined expression of the COVID-19-responsive genes in the ileum, colon and rectum CERTIFI cohort samples using geneset variation analysis (GSVA) and mixed linear modeling (gene~region * tissue type) was performed to compare expression between control, non-inflamed and inflamed samples. Box plots summarizing the mean expression (+/- SEM) of the two signatures are summarized in the upper and lower panels. Sample sizes are presented in Table S6. **B**. A heatmap summarizing the significance (-log adj P value) for the enrichment of genes Up- or Down- regulated following lung cell SARS-CoV2 infection in various IBD disease associated genesets derived from the MSCCR cohort analysis and IBD GWAS genes.

Figure S9: Subnetworks associated with COBID-19 response in hSIOs overlaps with NHBE-COVID-19 responsive subnetworks Two molecular expression signatures reflecting transcriptional responses to SARS-CoV-2 infection in human small intestinal organoids (hSIOs) were curated[28]. **A.** hSIOs cultured with differentiation media (DIF) contain predominantly enterocytes, goblet cells and low numbers of enteroendocrine cells. **B**. hSIOs grown in Wnt high expansion medium (EXP) consist mainly of stem cells and enterocyte progenitors. We determined expression of the hSIO COVID-19-responsive genes in the ileum, colon and rectum MSCCR cohort samples using geneset variation analysis (GSVA) and mixed linear modeling (gene~region*tissue type) was performed to compare expression between control, non-inflamed and inflamed samples. Box plots summarizing the mean expression (+/- SEM) of the two signatures are summarized in the upper and lower panels. P values are as indicated. **C**. A heatmap summarizing the significance (-log adj P value) for the enrichment of genes Up- or Down- regulated following iHIO SARS-

CoV2 infection in various IBD disease associated genesets derived from the MSCCR cohort analysis and IBD GWAS genes. **D**) A Venn diagram summarizing the overlaps of 3 subnetworks generated using the ileum CD BGRN, from projecting signatures associated with either 1. IBD-Inf; 2. NHBE_COVID-19 response or 3: hSIO (DIF media)-COVID-19 response, allowing 1 or 2 nearest neighboring genes. E). A Venn diagram summarizing the overlaps of 3 subnetworks generated using the ileum CD BGRN, from projecting signatures associated with either 1. IBD-Inf; 2. NHBE_COVID-19 response or 3: hSIO (EXP media)-COVID-19 response, allowing 1 nearest neighboring gene. The hSIO(DIF)- and hSIO(EXP)-COVID-19 associated subnetworks are found in Table S20. The intersecting genes are shown. Note many genes are also identified as KDGs in Figure 6e. The significance of the overlaps of various genesets is presented in each panel.

Supplementary Table Legends:

Table S1: Clinical characteristics of Non-IBD patients included in immunofluorescence analysis in Figure 1. Abbreviations: TI, terminal ileum; CRC, colorectal cancer; DM2, type 2 diabetes mellitus; HLD, hyperlipidemia; HTN, hypertension; GERD, gastroesophageal reflux disease; ED, erectile dysfunction; PUD, peptic ulcer disease; OA, osteoarthritis; BPH, benign prostatic hyperplasia; CAD, coronary artery disease; IBS, irritable bowel syndrome.

Table S2: Clinical characteristics of IBD patients included in immunofluorescence analysis in Figure S1. Clinical characteristics of IBD patients before (a) and/or after (b) biologic therapy. Macroscopic extent of disease refers to the Montreal classification for UC patients. Biologic naive is defined as no previous exposure to biologics. Abbreviations: SES-CD, Simple endoscopic score for Crohn Disease; 6MP, mercaptopurine; HBV, hepatitis B; HTN, hypertension; Afib, atrial fibrillation; CAD, coronary artery disease; GERD, gastroesophageal reflux disease; PPROM, preterm premature rupture of membranes; TI, terminal ileum.

Table S3: Clinical characteristics of IBD patients from the Mount Sinai Crohn's and Colitis Registry (MSCCR).

Table S4: Sample sizes associated with analysis in Figure 2a.

Table S5: Sample sizes associated with analysis in Figure 3.

Table S6: Sample sizes associated with analysis in Figure 4 and Figure S3.

Table S7: Subnetworks associated data in Figure 5a and 5d.

Table S8: Data associated with Figure 5c and f

Table S9: Data associated with Figure S5a

Table S10: Data associated with Figure S5b

Table S11: Data associated with Figure S5c

Table S12: Data associated with Figure S5d

Table S13: Data associated with Figure S6a

Table S14: Data associated with Figure S6c

Table S15: Data associated with Figure S7a

Table S16: Data associated with Figure S7b

Table S17: Data associated with Figure 6c networks

Table S18: Data associated with Figure 6c

Table S19: Data for Figure 6d

Table S20: Data for Figure S9d and e

Table S21: Data for Figure 6e (KDGs)

Table S22: Drug response associated CD ileum subnetworks

Table S23: Data for Figure 6f

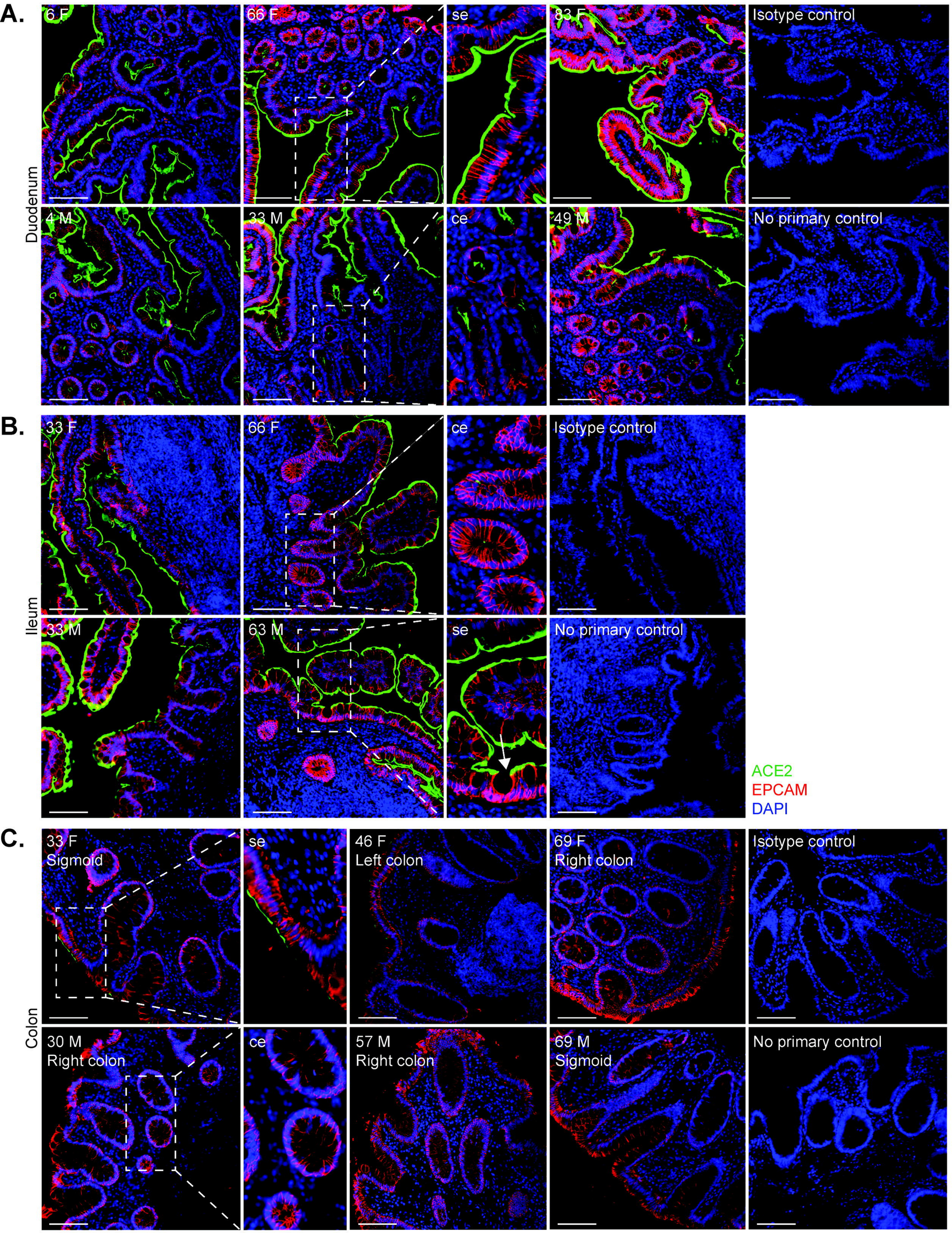
A.
Duodenum
6 F
66 F
se
83 F
Isotype control
4 M
33 M
ce
49 M
No primary control
B.
Ileum
33 F
66 F
ce
Isotype control
33 M
63 M
se
No primary control
ACE2
EPCAM
DAPI
C.
Colon
33 F
Sigmoid
se
46 F
Left colon
69 F
Right colon
Isotype control
30 M
Right colon
ce
57 M
Right colon
69 M
Sigmoid
No primary control

Figure 2

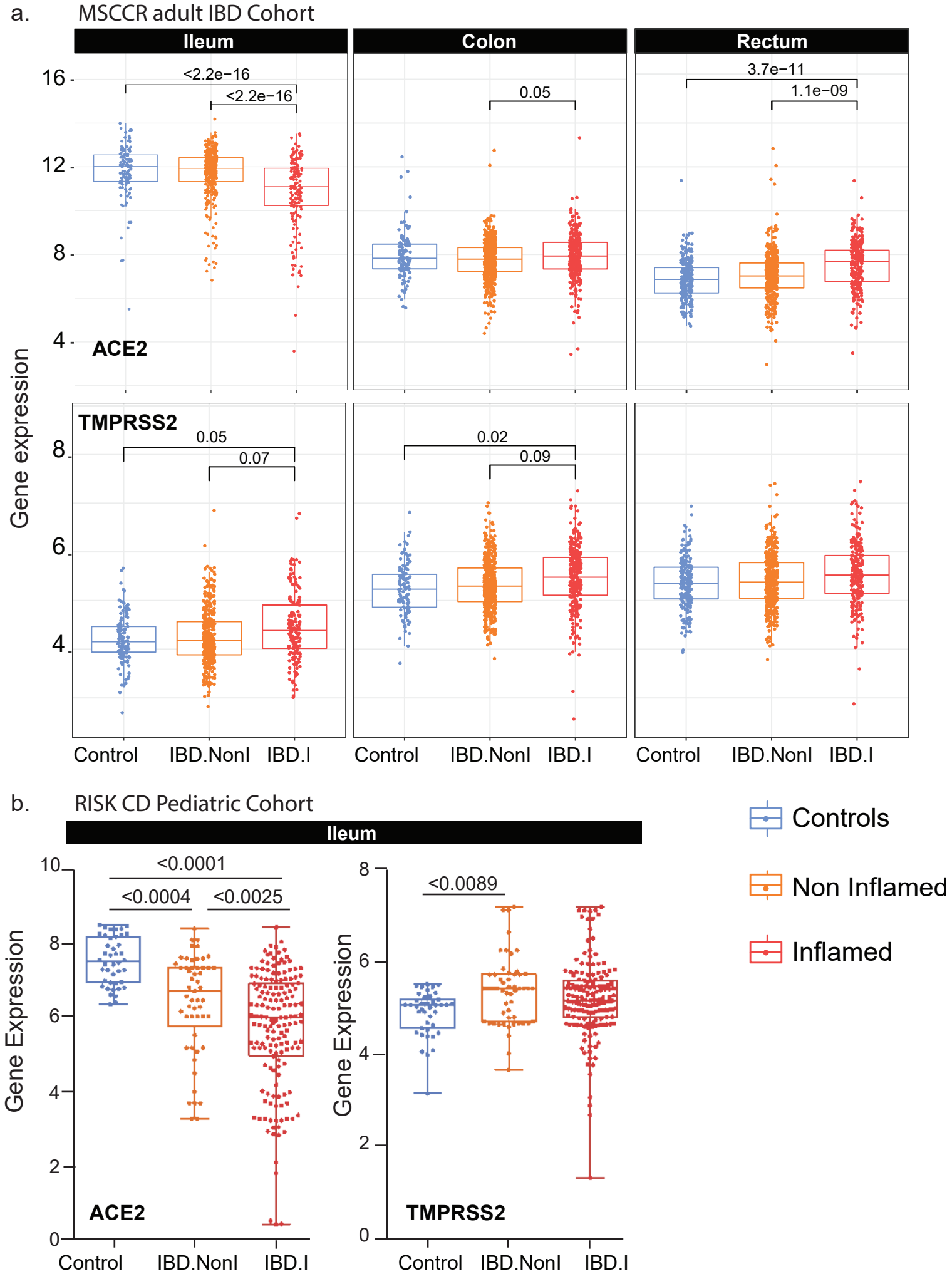
a.
MSCCR adult IBD Cohort
Ileum
Colon
Rectum
<2.2e−16
<2.2e−16
0.05
3.7e−11
1.1e−09
ACE2
TMPRSS2
0.05
0.07
0.02
0.09
Gene expression
Control
IBD.NonI
IBD.I
b.
RISK CD Pediatric Cohort
Ileum
<0.0001
<0.0004
<0.0025
<0.0089
Gene Expression
ACE2
TMPRSS2
Controls
Non Inflamed
Inflamed

Figure 3

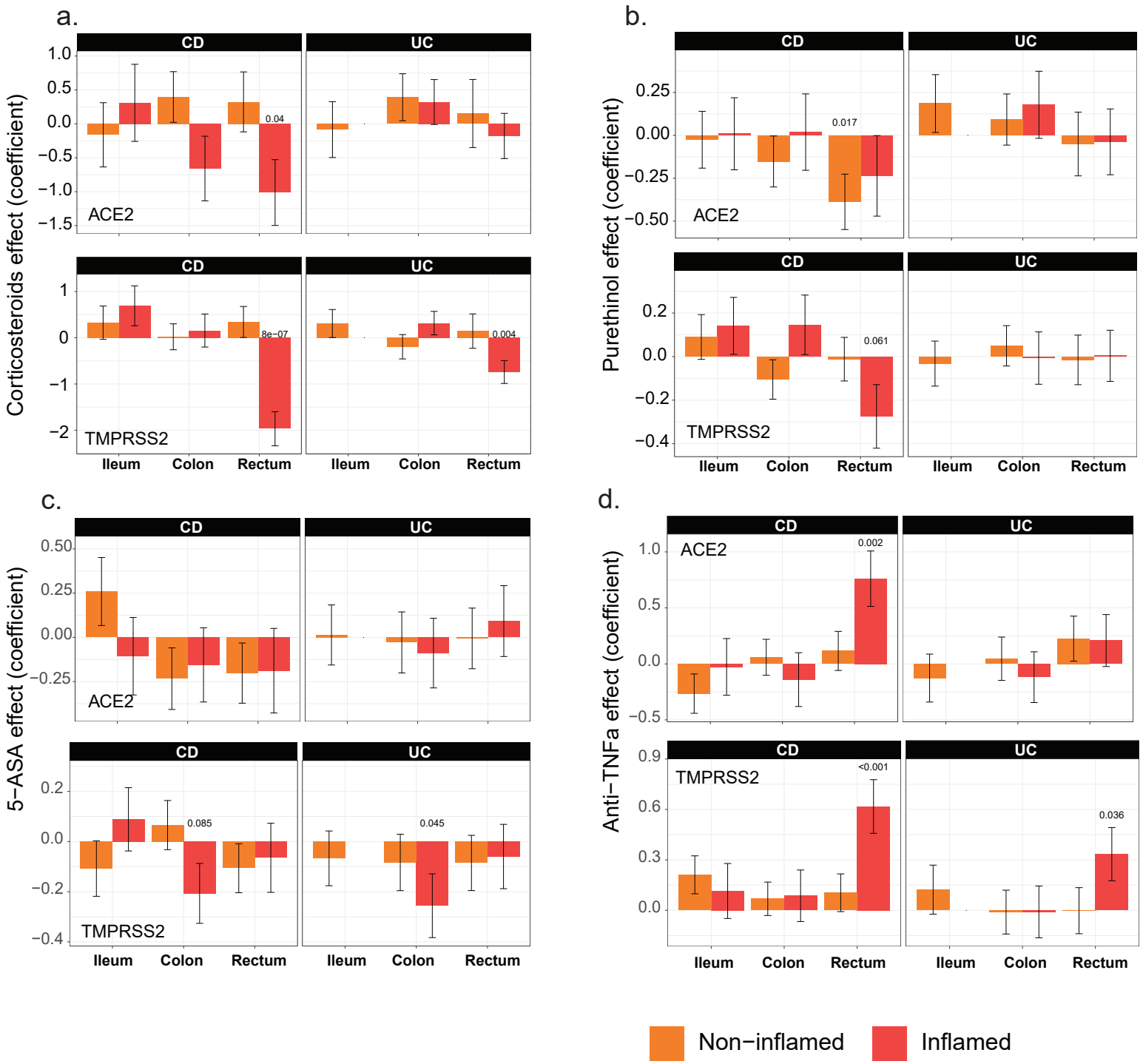
a.
b.
c.
d.
CD
UC
ACE2
TMPRSS2
Corticosteroids effect (coefficient)
Purethinol effect (coefficient)
5−ASA effect (coefficient)
Anti−TNFa effect (coefficient)
0.04
8e−07
0.004
0.017
0.061
0.085
0.045
0.002
<0.001
0.036
Ileum
Colon
Rectum
Non−inflamed
Inflamed

Figure 4

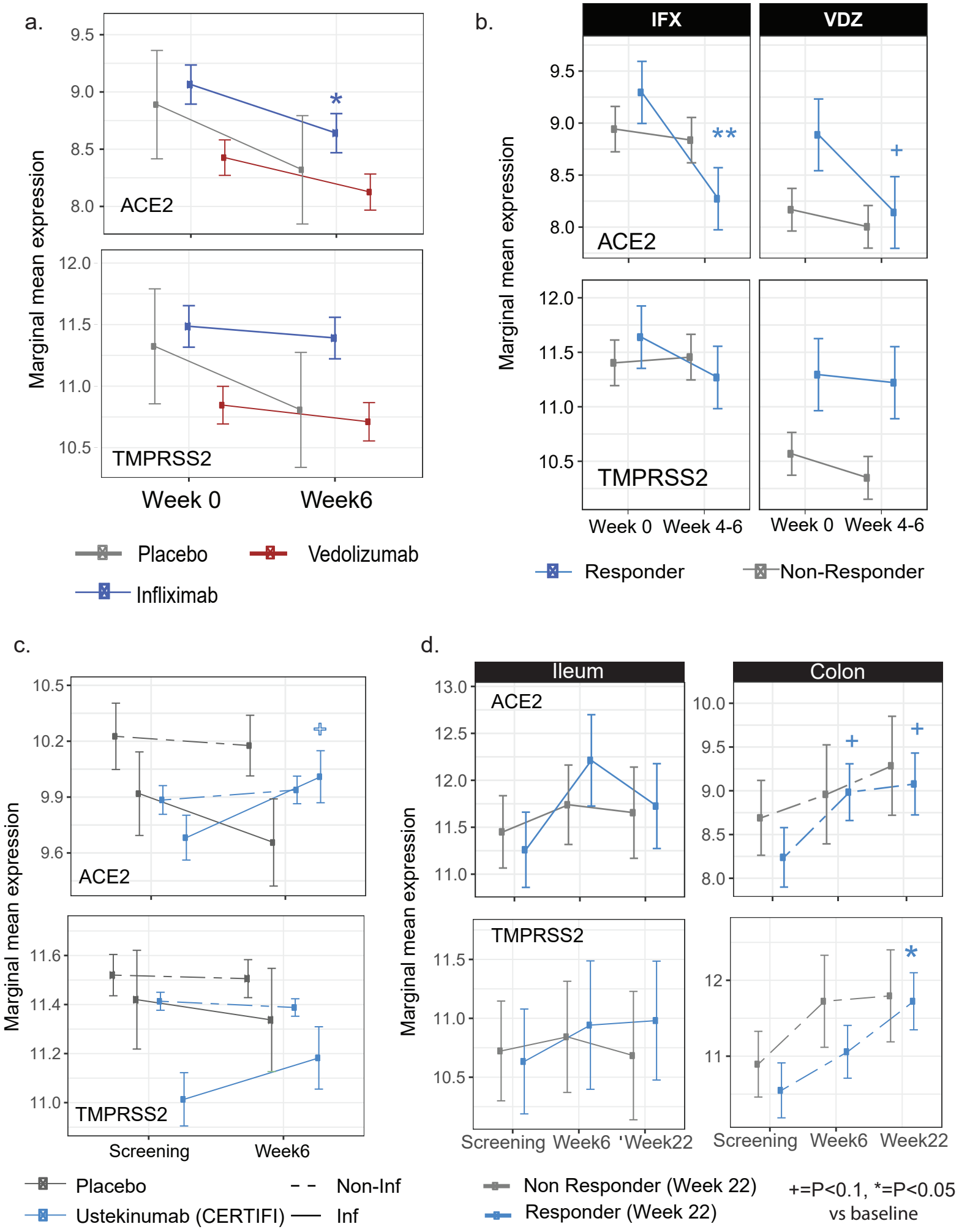
a.
Marginal mean expression
ACE2
TMPRSS2
Week 0
Week6
Placebo
Vedolizumab
Infliximab
b.
IFX
VDZ
Marginal mean expression
ACE2
TMPRSS2
Week 0
Week 4-6
Responder
Non-Responder
c.
Marginal mean expression
ACE2
TMPRSS2
Screening
Week6
Placebo
Ustekinumab (CERTIFI)
Non-Inf
Inf
d.
Ileum
Colon
Marginal mean expression
ACE2
TMPRSS2
Screening
Week6
Week22
Non Responder (Week 22)
Responder (Week 22)
+=P<0.1, *=P<0.05
vs baseline

Figure 5

a.

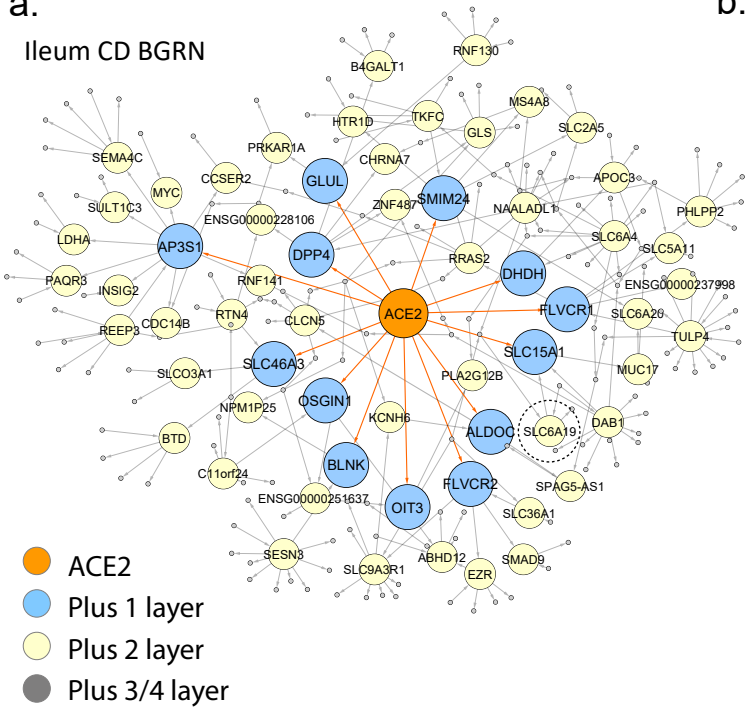

b.

ACE2 associated genes in 2 of 2 Ileum subnetworks

BEND7
CCT8P1
CD82
CHRNA7
CLCN5
EGFR-AS1
ENSG00000024595
ESPN
FADS6
GNA11
HAAO
HNRNPA1P9
JDP2
LRRC75A
MS4A8
MUC17
NBPF7
NSMF
NUCKS1
OIT3
PLB1
RHOU
SERPINA1
SLC15A1
SLC36A1
SLC7A7
SLC9A3R1
TCN2
TMEM117
TMEM150B

c.

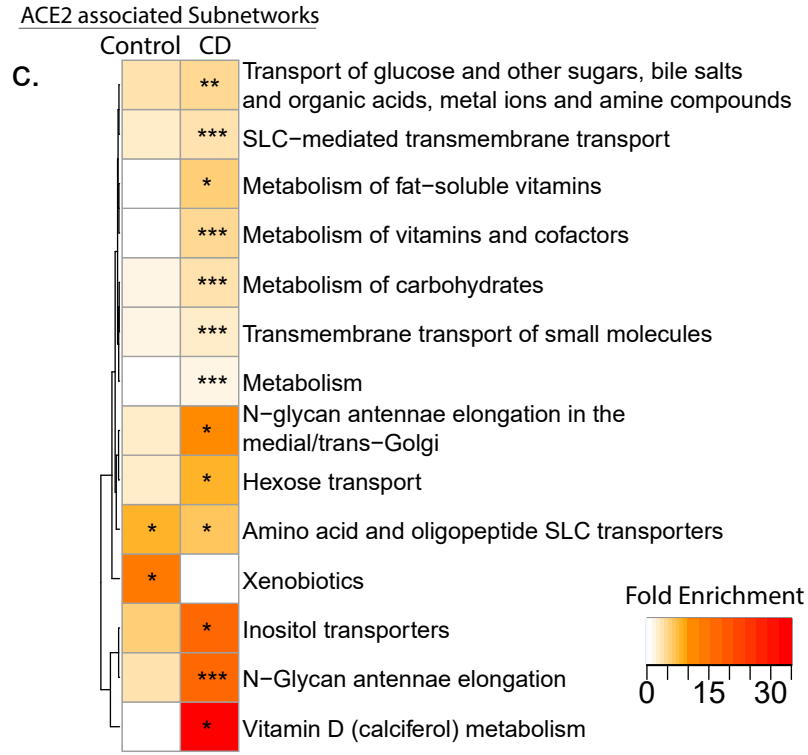

d.

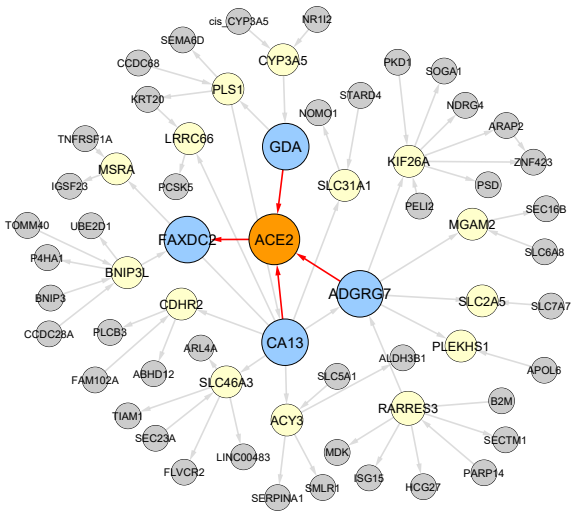

e.

ACE2 associated genes in 3 of 3 colon subnetworks

ACSL5
ACY3
ADGRG6
ANPEP
CA13
CNDP2
DGAT1
ENTPD7
MEP1B
MGAM2
PLEKHS1
SAT2
SEC16B
SLC46A3
SLC5A1
TKFC
TMEM92
UNC5CL

f.

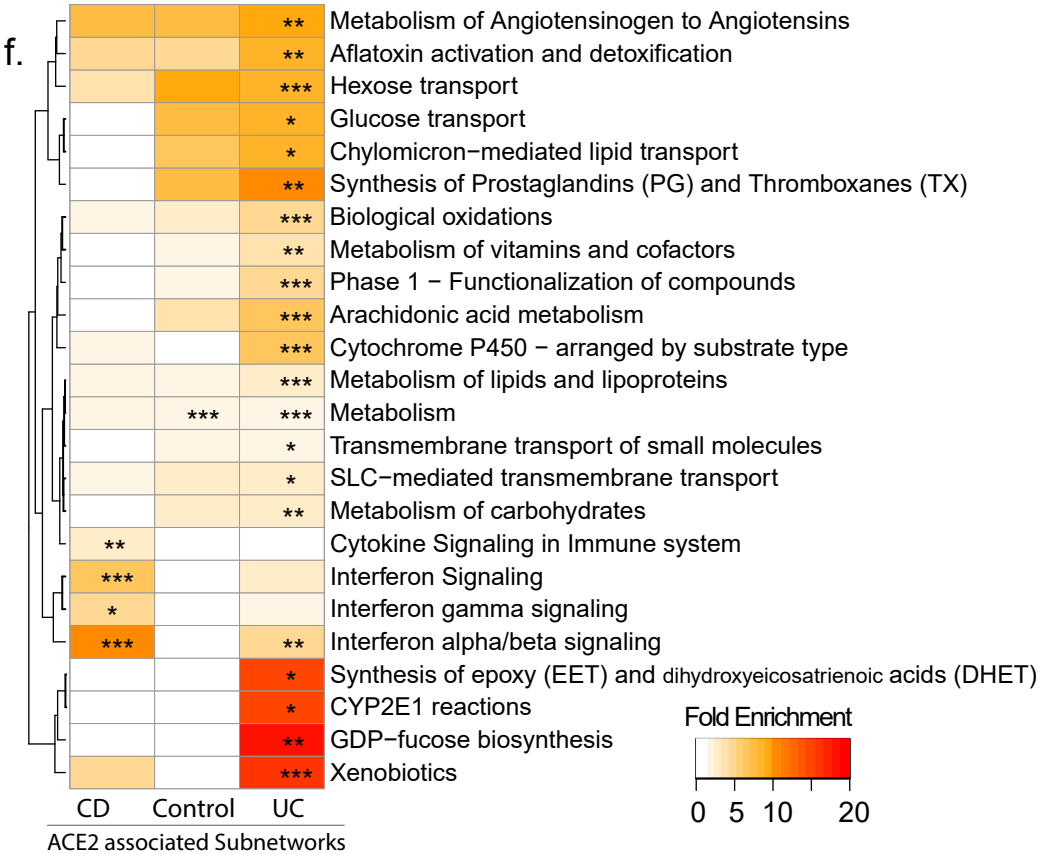

Adj P Value * = 0.1 -0.05, **=0.05-0.01, ***>0.01

Figure 6

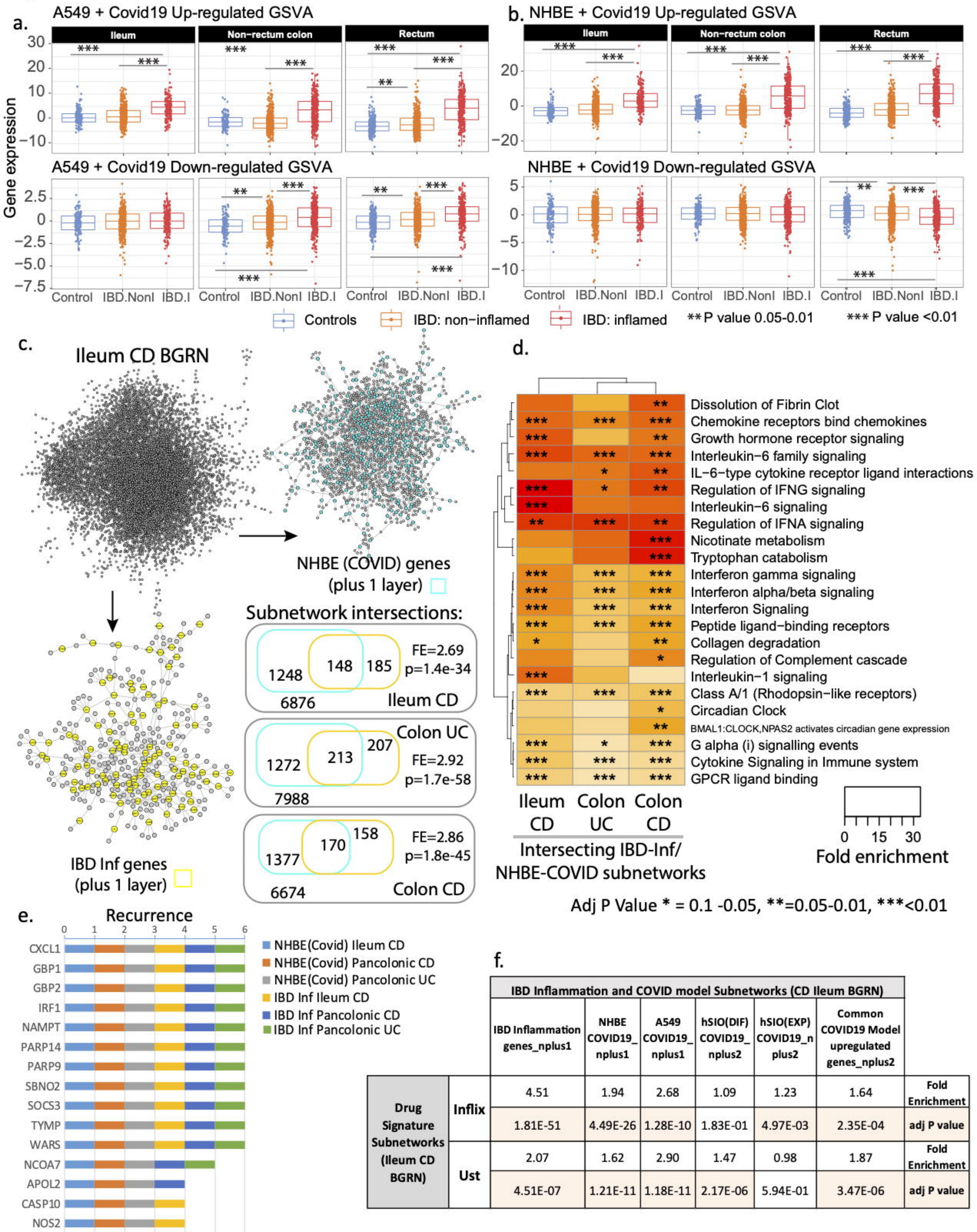

		IBD Inflammation and COVID model Subnetworks (CD Ileum BGRN)						
		IBD Inflammation genes_nplus1	NHBE COVID19_ nplus1	A549 COVID19_ nplus1	hSIO(DIF) COVID19_ nplus2	hSIO(EXP) COVID19_n plus2	Common COVID19 Model upregulated genes_nplus2	
Drug Signature Subnetworks (Ileum CD BGRN)	Inflix	4.51	1.94	2.68	1.09	1.23	1.64	Fold Enrichment
		1.81E-51	4.49E-26	1.28E-10	1.83E-01	4.97E-03	2.35E-04	adj P value
	Ust	2.07	1.62	2.90	1.47	0.98	1.87	Fold Enrichment
		4.51E-07	1.21E-11	1.18E-11	2.17E-06	5.94E-01	3.47E-06	adj P value